Simulations of Rapid Compression Machines:
Validation of OpenFOAM as adopted library

If you have any question on this presentation, don't hesitate to contact me by email (fcontino@vub.ac.be).

CFD simulations of
Rapid Compression Machines

Nicolas Bourgeois, Francesco Contino

22nd of November, 2017

The objective of this short presentation is to provide a succinct demonstration of the ability of the OpenFOAM tools to perform properly non-reactive CFD and 0-D simulations of Rapid Compression Machines (RCMs).

RANS axi-symmetric results based on a geometry similar to the Argonne RCM

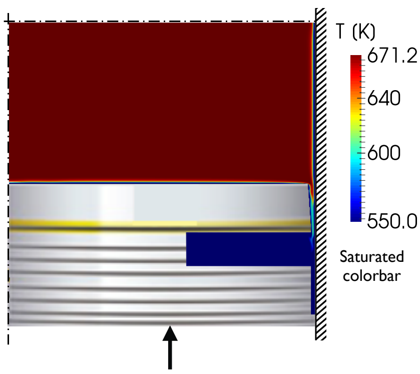

2

The Argonne RCM is chosen as a baseline case, but similar conclusions should be drawn for any other RCM. CFD results are based on RANS simulations and a 2-D axisymmetric mesh. Piston is moving upwards (here a visualization of the temperature field at the end of the compression).

RANS simulations of the Argonne RCM using OpenFOAM:

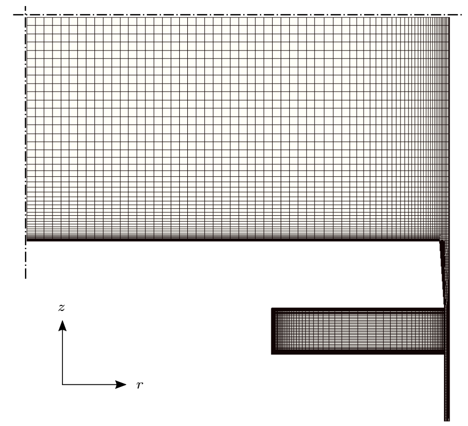

~31,800 cells at BDC
~9,000 cells at TDC

3

The number of cells in the compressive direction decreases with time to keep an acceptable aspect ratio for the cells. Typically, there are around 32,000 cells at the beginning and 9,000 cells at the end of the compression.

Piston trajectory is used as an input (old version of the trajectory, with an improved deceleration since then)

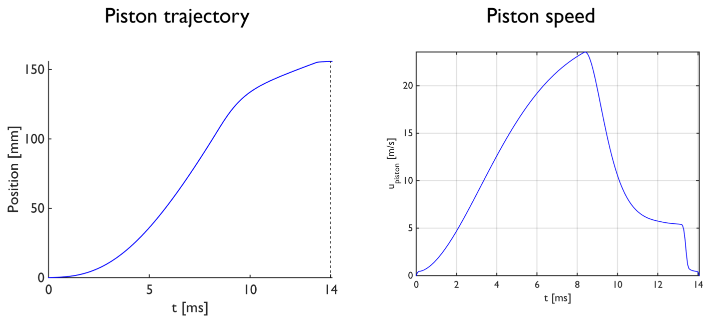

4

The piston trajectory needs to be provided by the user. Left: (former) piston trajectory of the Argonne RCM. Right: corresponding piston speed profile.

1) 0-D adiabatic computation based on Janaf coefficients

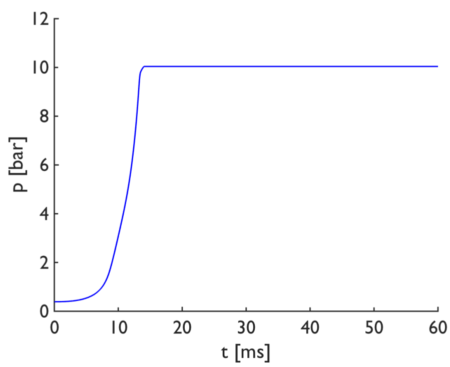

$$p_0 = 0.39 \text{ bar}$$
$$T_0 = 303.85 \text{ K}$$

$0.846\ N_2,\ 0.119\ O_2,\ 0.034\ nC_7H_{16}$

5

This is a “ĂIJhandmade”Ăİ adiabatic computation (performed with MATLAB).

2) 0-D adiabatic simulation in OpenFOAM

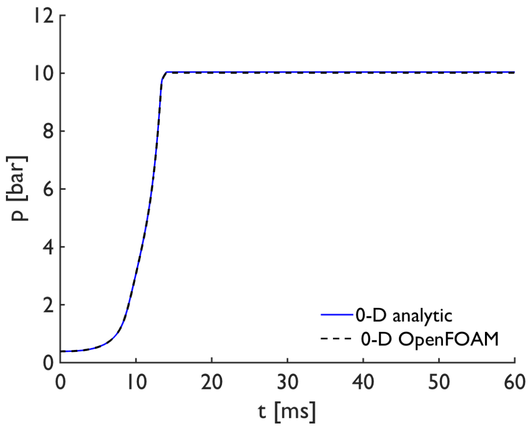

6

As it should, comparison is almost perfect with an OpenFOAM 0-D simulation.

2) 0-D adiabatic simulation in OpenFOAM

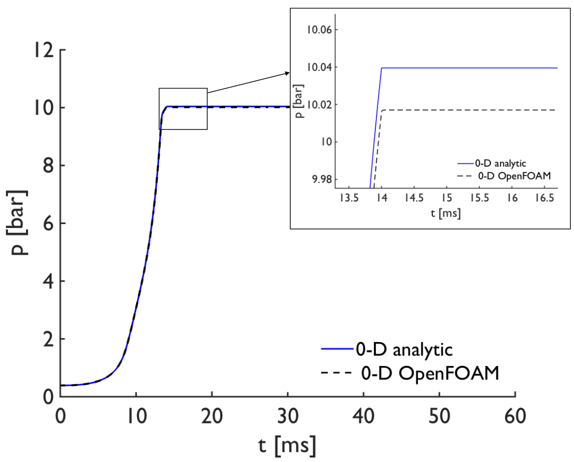

7

The difference is around 0.2% and may be attributed to the integration schemes that are not equivalent for both computations.

3) 2-D adiabatic with a flat piston: coarse mesh

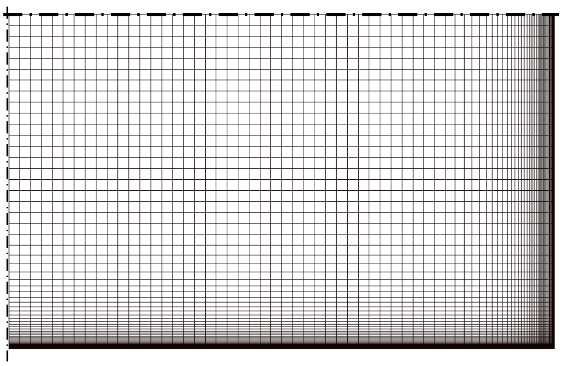

5,200 cells at TDC

8

A 2-D adiabatic simulation is supposed to give the exact same pressure curve, regardless of the mesh refinement.

3) 2-D adiabatic with a flat piston: coarse mesh

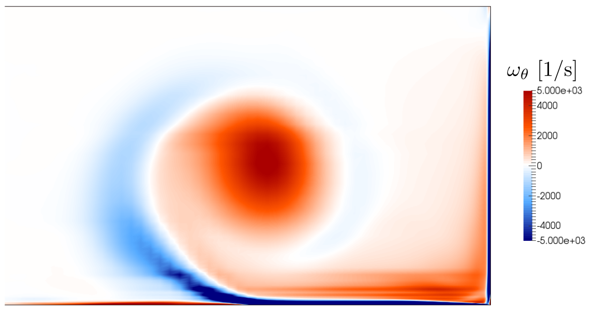

End of the compression

By the way, it is interesting to notice that the vortex roll-up is not avoided in adiabatic conditions. Hence, the vortex roll-up is not primarily driven by thermal boundary layers but by the wall vorticity that rolls up during the compression.

9

3) 2-D adiabatic with a flat piston: coarse mesh

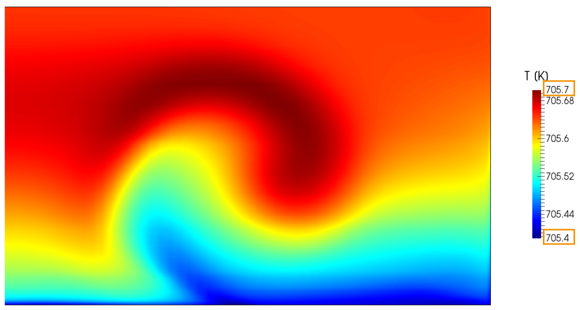

The temperature field is almost perfectly homogeneous, as it should. Differences might be attributed to the fact that the compression is adiabatic but not isentropic: some friction on the walls alters possibly (very slightly) the temperature field.

10

3) 2-D adiabatic with a flat piston: coarse mesh

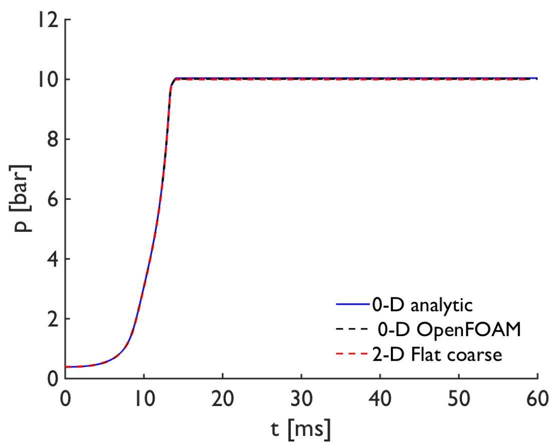

The differences on the pressure traces are minor.

11

3) 2-D adiabatic with a flat piston: fine mesh

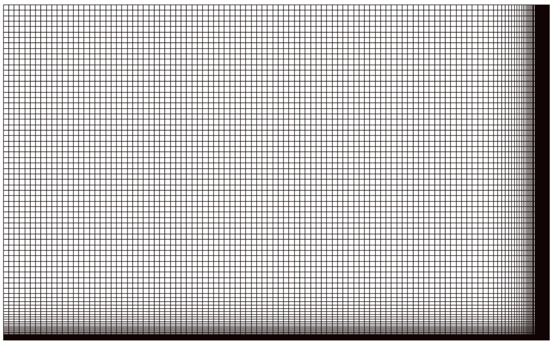

13,400 cells at TDC

12

We try the same exercise with a finer mesh.

3) 2-D adiabatic with a flat piston: fine mesh

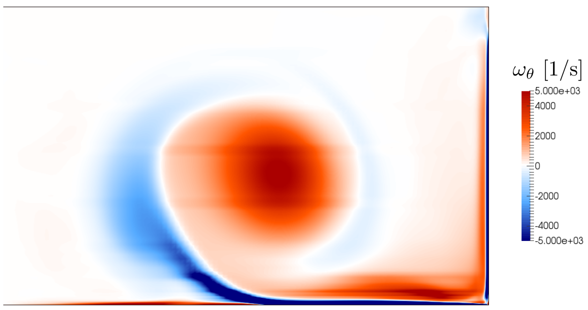

End of the compression

13

It it also interesting to observe that the flow patterns of the rolled-up vortex are not strictly equivalent to that of the coarser mesh (cfr. slide 9), suggesting that an accurate capture of the vortex roll-up phenomenology requires a high level of mesh refinement (more than if the objective is restricted to the capture of the pressure history).

3) 2-D adiabatic with a flat piston: fine mesh

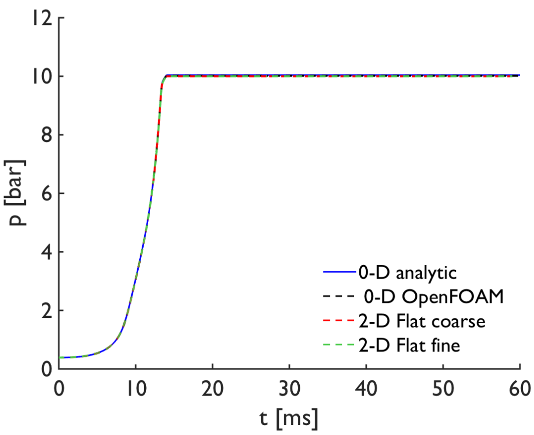

14

Differences on the pressure traces are not significant.

4) 2-D adiabatic with a creviced piston

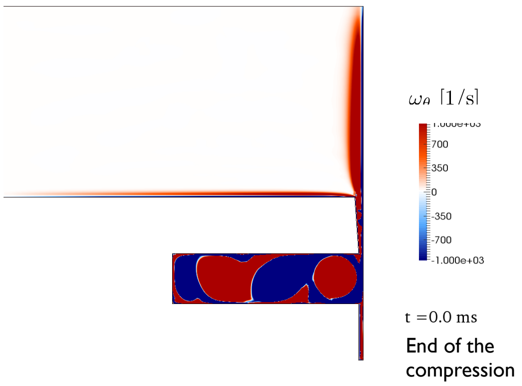

15

Using a piston with appropriate crevice avoids the formation of the vortex during the compression. . . Ăę

4) 2-D adiabatic with a creviced piston: vortex roll-up in the post-compression phase

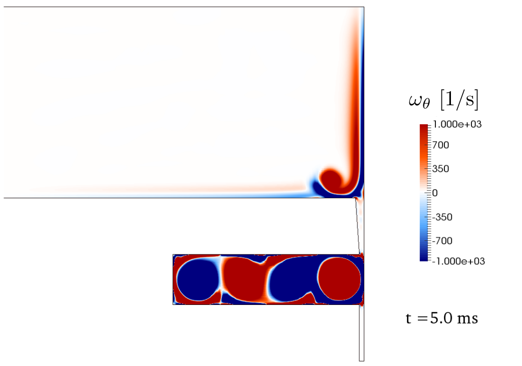

16

. . . still it does not prevent it during the post-compression period. Indeed, as the mass transfer between the main reaction chamber and the crevice volume stops once the piston is at rest, the residual wall vorticity present on the cylinder liner cannot be transferred anymore to the crevice. As a consequence, there is a votex roll-up, very similar to the one observed when implementing the crevice containment concept. In a real RCM, mass keeps to be moved from the chamber to the crevice, even when the piston stops.

4) 2-D adiabatic with a creviced piston: vortex roll-up in the post-compression phase

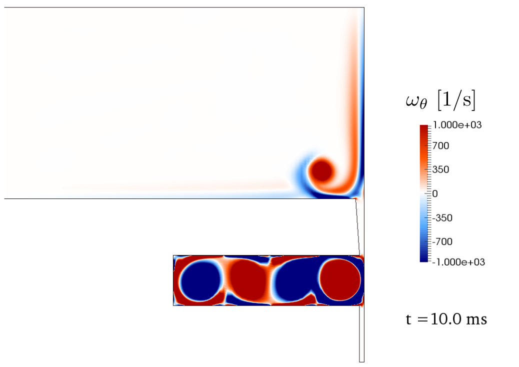

17

4) 2-D adiabatic with a creviced piston

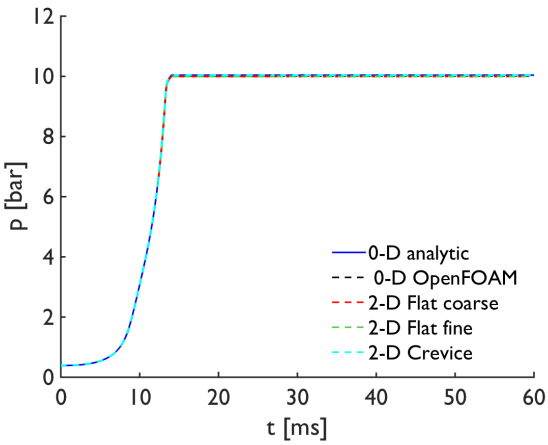

18

Still, there is no reason to observe differences on the pressure traces.

4) 2-D adiabatic with a creviced piston

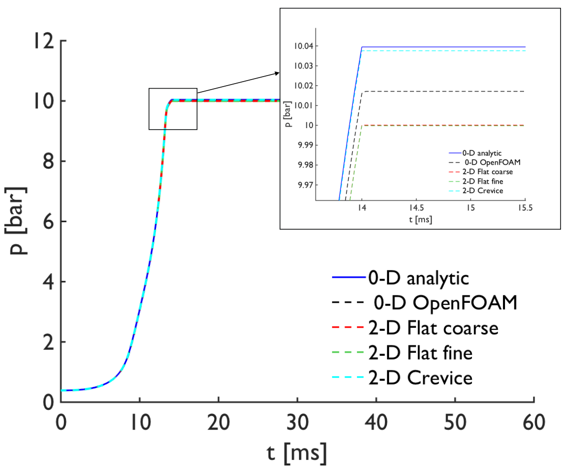

19

Differences do not exceed 0.4%, which seems acceptable. If better performances need to be achieved, further investigation about the exact reasons of the observed discrepancies should be undertaken. However, it can be mentioned that even apparently insignificant differences on the geometrical compression ratios between the different cases may have significant consequences on the final pressure after compression. This could be the main reason explaining those differences (to be confirmed).

Temperature curves for all cases

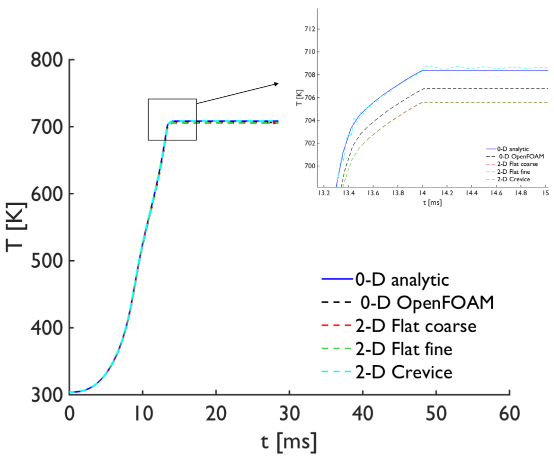

20

All values shown here are averaged values inside the geometries. They are almost equal to core temperatures as the temperature field is almost perfectly homogeneous, hence 0-D cases may be compared to 2-D cases. Differences are minor and may be attributed to the same factors as those described below (essentially, differences in terms of geometrical compression ratios).